Available online at www.sciencedirect.com
ScienceDirect
Developmental Biology 297 (2006) 387–401
DEVELOPMENTAL BIOLOGY
www.elsevier.com/locate/ydbio

# Position and time specify the migration of a pioneering population of olfactory bulb interneurons

Eric S. Tucker [a], Franck Polleux [b], Anthony-Samuel LaMantia [a,*]

[a] *Department of Cell and Molecular Physiology, UNC Neuroscience Center, The University of North Carolina at Chapel Hill School of Medicine, Chapel Hill, NC 27599, USA*

[b] *Department of Pharmacology, UNC Neuroscience Center, The University of North Carolina at Chapel Hill School of Medicine, Chapel Hill, NC 27599, USA*

Received for publication 20 March 2006; revised 29 April 2006; accepted 5 May 2006
Available online 19 May 2006

**Abstract**

We defined the cellular mechanisms for genesis, migration, and differentiation of the initial population of olfactory bulb (OB) interneurons. This cohort of early generated cells, many of which become postmitotic on embryonic day (E) 14.5, differentiates into a wide range of mature OB interneurons by postnatal day (P) 21, and a substantial number remains in the OB at P60. Their precursors autonomously acquire a distinct identity defined by their position in the lateral ganglionic eminence (LGE). The progeny migrate selectively to the OB rudiment in a pathway that presages the rostral migratory stream. After arriving in the OB rudiment, these early generated cells acquire cellular and molecular hallmarks of OB interneurons. Other precursors – including those from the medial ganglionic eminence (MGE) and OB – fail to generate neuroblasts with similar migratory capacity when transplanted to the LGE. The positional identity and migratory specificity of the LGE precursors is rigidly established between E12.5 and E14.5. Thus, the pioneering population of OB interneurons is generated from spatially and temporally determined LGE precursors whose progeny uniquely recognize a distinct migratory trajectory.


*Keywords:* Migration; Interneuron; Olfactory bulb; Development; Forebrain; Neurogenesis; Ganglionic eminence; Rostral migratory stream

## Introduction

The production, migration, and differentiation of the earliest generated OB interneurons have largely been unexplored, despite considerable attention to the genesis of these cells during early postnatal life and adulthood (Hinds, 1968a; Rosselli-Austin and Altman, 1979; Bayer, 1983; Lois and Alvarez-Buylla, 1993; Luskin, 1993; Lois and Alvarez-Buylla, 1994; Alvarez-Buylla and Lim, 2004). Genetic loss-of-function and fate mapping studies (Corbin et al., 2000; Wichterle et al., 2001; Yun et al., 2001, 2003) clearly demonstrate that precursors in the LGE produce progeny that migrate into the rudimentary OB and differentiate into OB interneurons. The cellular and molecular specificity of this population, however, has not been defined. Moreover, it is unclear whether the earliest cohort of cells from the LGE migrate along a specific pathway to the OB rudiment and differentiate into a full range of OB interneurons that persist throughout life, perhaps as a scaffold upon which the adult compliment is established postnatally and replaced thereafter. Finally, it is not known when the production of embryonic OB interneurons becomes restricted to the LGE during development. Accordingly, we used in vivo neuronal birth dating, molecular labeling, and a novel in vitro assay to determine the identity of embryonically generated OB interneurons and their precursors, and define their migratory route to the rudimentary OB.

Concurrent with the production of presumptive OB interneurons in the LGE, precursors in the adjacent MGE generate cortical, striatal, and hippocampal interneurons (Anderson et al., 1997; Marin et al., 2000; Pleasure et al., 2000; Anderson et al., 2001; Wichterle et al., 2001). The extent to which position in the ganglionic eminences controls specific aspects of neuronal identity, such as the selection of migratory pathways and differentiation programs, remains unclear. Previous reports

* Corresponding author. Fax: +1 919 966 6927.
*E-mail address:* anthony_lamantia@med.unc.edu (A.-S. LaMantia).

0012-1606/$ - see front matter © 2006 Elsevier Inc. All rights reserved.
doi:10.1016/j.ydbio.2006.05.009

indicate that precursors from the LGE, MGE, and caudal ganglionic eminence (CGE) display a significant degree of intrinsic determination (Wichterle et al., 1999; Wichterle et al., 2001; Nery et al., 2002; Yozu et al., 2005); nevertheless, the immediate influence of extrinsic factors available in each location is unknown. We therefore used our novel in vitro whole telencephalon assay, which preserves the in vivo architecture of the developing forebrain, to ask whether autonomous factors or local signals within the LGE distinguish OB interneuron precursors and influence their subsequent migration and differentiation.

We found that OB interneuron precursors in the LGE are positionally specified and autonomously acquire a distinct migratory capacity between E12.5 and E14.5. These precursors give rise to a heterogeneous population of stable OB interneurons. Local LGE or MGE cues are insufficient to reprogram the migratory fate of heterologous precursors; nevertheless, position in the LGE is required for significant migration of LGE cells into the OB rudiment. Apparently, patterning mechanisms that establish distinct domains in the ventral forebrain confer LGE precursors with the unique ability to migrate to the OB and acquire distinctive characteristics associated with OB interneurons.

## Materials and methods

### *Animals*

Wild-type Institute of Cancer Research (ICR) mice and mice hemizygous for a Enhanced Yellow Fluorescent Protein (EYFP) gene under control of the chicken beta actin promoter/cytomegalovirus immediate early enhancer [TgN (ActbEYFP)1Nagy (Jax 003772)] were maintained by the University of North Carolina at Chapel Hill Department of Laboratory Animal of Medicine. Wild-type females were paired with hemizygous EYFP males to generate timed pregnancies (day of vaginal plug = E0.5). Timed-pregnant mice were sacrificed by rapid cervical dislocation, and embryos harvested for tissue culture or fixed for immunocytochemical analysis. Adult animals used for immunocytochemistry were deeply anesthetized with urethane (2 mg/kg) and perfusion fixed. All experimental procedures were reviewed and approved by the UNC-CH Institutional Animal Care and Use Committee.

### *Bromodeoxyuridine administration*

Timed-pregnant mothers were injected intraperitoneally on E14.5 with 5-bromo-2-deoxyuridine (BrdU; Sigma, St. Louis, MO; dissolved in 0.9% NaCl with 0.07 N NaOH) at 50 mg/kg followed by an intraperitoneal injection of thymidine 1 h later (Sigma, St. Louis, MO; 500 mg/kg, dissolved in 0.9% NaCl with 0.07 N NaOH) to limit availability of BrdU to mitotically active cells to a brief interval. Litters were harvested 6-h post BrdU injection for the E14.5 time point and each subsequent day from E15.5 to postnatal day 0 (P0). For long-term analyses, E14.5 timed-pregnant animals were injected intraperitoneally with a single 50 mg/kg dose of BrdU, and mice from those litters were sacrificed on P21 and P60.

### *Tissue preparation*

Embryonic brains (up to E17.5) were dissected in Dulbecco's phosphate-buffered saline (PBS; pH = 7.4) and immersion fixed overnight in 4% paraformaldehyde in PBS (pH = 7.4). E18.5 embryos and P0 pups were perfused in the same fixative and brains postfixed 2 h at RT. P21 and P60 mice were perfused with 4% paraformaldehyde in 0.1 M phosphate buffer, 4% sucrose (pH = 7.4). Fixed brains were rinsed through graded sucrose solutions (10%–30%), embedded in agar, and frozen in cryo-embedding compound (OCT) using liquid-nitrogen-cooled 2-methyl-butane. These blocks were stored at −80°C, and 12-μm cryosections were cut at −20°C.

### *Immunocytochemistry*

Sections were rehydrated in PBS, incubated in 2 N HCl for 30 min at 37°C, rinsed 3 × 15 min in a 3.8% sodium borate solution (pH = 8.5), 2 × 10 min in PBS and then incubated for 1.5 h in 3% bovine serum albumin (BSA), 10% normal goat serum (NGS), 0.3% Triton X-100, and 0.1% sodium azide. Mouse anti-BrdU (1:100; Beckton Dickinson) was diluted in the BSA/Triton-X/Azide solution with 1% NGS and incubated for 48 h at 4°C. For double-labeling experiments, the following rabbit polyclonal antibodies were used: rabbit anti-GABA (1:1000–1:4000; Sigma), rabbit anti-calretinin (1:1000; Chemicon), rabbit anti-calbindin (1:1000; Chemicon), and rabbit anti-tyrosine hydroxylase (1:500; Chemicon). Appropriate dilutions of these antibodies were added to the mouse anti-BrdU for approximately 24 of the 48-h incubation, except for rabbit anti-calbindin, which was incubated for the full 2 days. The sections were next incubated for 2 h at RT with goat anti-mouse Alexa 488 (1:4000; Molecular Probes) and goat anti-rabbit Alexa 546 (1:2000; Molecular Probes). Secondary antibodies were diluted in BSA/Triton-X/Azide with 1% NGS. Sections were counterstained with *bis*-benzamide, and cover-slipped with Mowiol + PPDA to retard photobleaching.

### *Quantification of immunocytochemically labeled OB interneurons*

P21 brains, harvested from animals receiving BrdU at E14.5, were serially sectioned into 4 separate horizontal series spanning the entire dorsal–ventral axis of the OB. Three sets of four series (one series for each marker), collected from three independent animals, were used. 5 evenly spaced sections from each series were chosen for photo-documentation and counting. Montages were constructed in Adobe Photoshop, and lines representing laminar divisions were drawn on each montage. On each section, 6 non-overlapping radial probes (ventricular to pial surface) were made along the anterior–posterior axis of the OB (see Fig. 2A). In each probe, $BrdU^+$ cells in each laminar division were counted. Double-labeled $BrdU^+$ cells were also counted in each layer. The total numbers of $BrdU^+$ cells and BrdU-double-labeled cells, for each layer, were summed across all three brains and percentages of $BrdU^+$ cells co-expressing each marker calculated.

### *Whole-telencephalon cultures*

We adapted an approach described previously (Polleux and Ghosh, 2002), to establish our E14.5 whole-telencephalon cultures. E14.5 $EYFP^+$ embryos were sorted from wild-type littermates and transferred to ice-cold complete Hank's balanced salt solution (complete HBSS) without sodium bicarbonate but with 9 mM HEPES and 0.001% phenol red at pH = 7.4. Brains were dissected in ice-cold complete HBSS. After removing the pia from wild-type forebrains, cuts were made with a microscalpel blade to facilitate flattening of each telencephalon. Cortices were cut into approximate thirds: one cut was made above the OB, and two dorsal cuts were made at opposite poles of the cortical hem (see Fig. 3A). Two cuts flanking the rostral and caudal aspects of the septum were also made. These hemi-forebrains were transferred to laminin/poly-lysine-coated 6-well inserts (Falcon) and oriented with their ventricular surfaces facing upwards. LGE and MGE grafts, as well as grafts from the OB and ventral spinal cord, were dissected from $EYFP^+$ brains and stored separately in ice-cold complete HBSS. Fine forceps were used to make small openings in either the LGE or MGE, and $EYFP^+$ LGE or MGE grafts were transferred to a host telencephalon with a micropipette. After grafts were positioned, the ventricular surface of cut forebrains was filled with complete HBSS to unfold cortical and septal flaps and flatten them upon the filter surface. These cultures were grown for 4 days at 37°C/95% $O_2$/5% $CO_2$ in 1.8 ml of Slice Culture Medium (as described previously) supplemented with 5% heat-inactivated horse serum (Sigma) and 10 mM HEPES; media were exchanged after 2 days.

### Explant cultures

Mesenchymal/Epithelial co-cultures were prepared as previously described (LaMantia et al., 2000). E9.5 EYFP$^+$ ventrolateral forebrain was microdissected, and frontonasal mesenchyme was removed by enzymatic digestion. This epithelium was directly transplanted into E14.5 LGE, cultured alone, or with wild-type frontonasal mesenchyme. Explants were grown floating on Millipore filters in DMEM/10%FBS for 2 days at 37°C/95% $O_2$/5% $CO_2$. After 2 days in vitro, isolated forebrain epithelium or forebrain epithelium co-cultured with wild-type frontonasal mesenchyme was transplanted into the E14.5 LGE. The M/E co-cultures were enzymatically digested, and the mesenchyme removed prior to grafting.

### Whole-mount immunocytochemistry

Whole-telencephalon cultures were fixed at RT for 2 h or overnight at 4°C with 4% paraformaldehyde in PBS. Tissue was rinsed in PBS and blocked in permeability solution (Polleux and Ghosh, 2002) with 5% normal goat serum (NGS) overnight at 4°C. Rabbit anti-GFP (1:2000; Molecular Probes) and mouse primary antibodies were applied overnight at 4°C. After rinsing in PBS, goat anti-rabbit Alexa 488 (1:4000; Molecular probes) and goat anti-mouse Alexa 546 (1:2000; Molecular probes) were applied simultaneously overnight at 4°C. Tissue was rinsed in PBS, cleared in hypaque (Amersham) and mounted onto slides. The following primary antibodies were used with the rabbit anti-GFP antibody: mouse anti-Tuj1 (1:1600; Covance); mouse anti-Calretinin (1:1000; Chemicon); mouse anti-GAD-6 (1:500; Developmental studies hybridoma bank); mouse anti-MAP-2 (1:500; Sigma); mouse anti-neurofilament 165 (2H3) (1:5000; Developmental studies hybridoma bank); rabbit anti-GABA (1:4000; Sigma) was used alone.

### Quantification and statistical analysis of migration

For all experiments, seven independent whole-telencephalon preparations were evaluated quantitatively for each transplant configuration. For grafts placed in the LGE, three non-overlapping fields in the OB and cortex, equidistant from the graft site, were imaged with a confocal microscope. Similarly, three non-overlapping fields in the OB and dorsal LGE (equidistant from the MGE graft site) were imaged for grafts placed in the MGE. Each field represented a 20 μm z-stack collected at an interval of 1 μm with a 40× objective. Confocal z-stacks were maximally projected, and EYFP$^+$ cells were counted in each field. For each experiment, the total numbers of EYFP$^+$ cells were recorded for each field and analyzed by two-way ANOVA. The independent variables used in our two-way ANOVA analyses were (1) the transplant configuration (homotopic versus heterotopic) and (2) the target destination (OB versus Cortex; OB versus dorsal LGE). All reported $P$ values represent the statistical probabilities of an interaction between these two independent variables.

### Microscopy

Macroscopic images, bright field and fluorescent, of live or fixed preparations were collected with a 4 Mega pixel Nikon digital camera mounted on a Leica MZFLIII dissecting microscope. Fluorescently labeled cryosections were imaged on a Leica DMR microscope at 20× or 40×. Epifluorescent images were acquired with a cooled CCD camera (Hamamatsu ORCA) using OpenLab

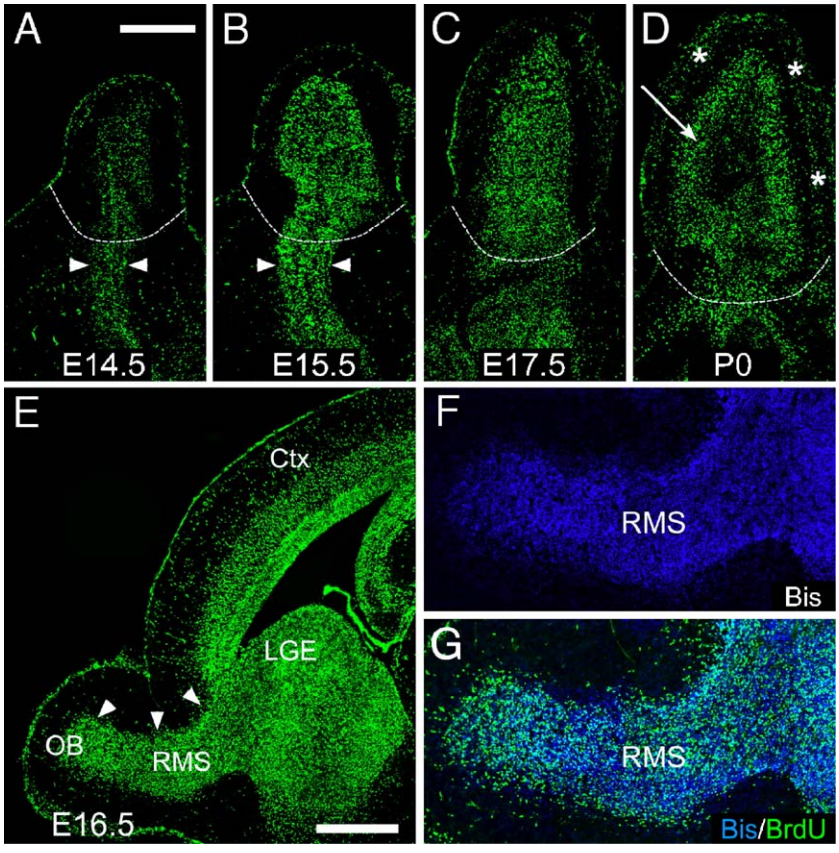


Fig. 1. Cells labeled with BrdU on E14.5 migrate into the developing OB. (A) BrdU$^+$ cells are present in the OB rudiment (above dashed line) and along the anterior horn of the lateral ventricle (arrowheads) after 6 h. (B) One day later, BrdU$^+$ cells accumulate in the OB and along the rostral extension of the lateral ventricle (arrowheads). (C) After 3 days, BrdU$^+$ cells continue to fill the core of the OB as it enlarges. (D) By P0, BrdU$^+$ cells occupy the nascent glomerular (asterisks) and granule cell (arrow) layers of the OB. (E) BrdU$^+$ cells are present in a continuous stream (arrowheads) extending from the anterior margin of the lateral ventricle to the OB rudiment at E16.5. (F–G) Nucleic acid counterstain (F; *bis*-benzamide) reveals that BrdU$^+$ cells fill a cell-dense pathway (G) resembling the adult rostral migratory stream. Scale bar in panels A and E = 500 μm, scale bar in panel A applies to panels B–D. OB = olfactory bulb; Ctx = cortex; RMS = rostral migratory stream.

(Improvision) image acquisition software. Fluorescently labeled whole-mount preparations were imaged on a Zeiss LSM 510 upright confocal microscope (UNC Neuroscience Center Confocal Microscopy Core) equipped with Argon and Green HeNe lasers. Red and green fluorophores were simultaneously collected on separate channels. For low-power montages, maximum projections were made from 6-μm serial optical sections collected with a 10× Plan-Neofluar objective. For high-power images, 0.5–1 μm serial optical sections were collected with either a 40× Plan-Neofluar or a 63× Plan-Apochromat oil immersion objective with up to 2× digital zoom. Images were adjusted for brightness, contrast, and intensity in Adobe Photoshop.

## Results

### *Early genesis and migration of ventral forebrain cells to the OB*

Birth dating studies suggest that most granule and periglomerular cells in the mouse OB are generated between E18 and P5 (Hinds, 1968a). Nevertheless, there is significant evidence that LGE precursors produce OB interneurons before E18 (Toresson and Campbell, 2001; Wichterle et al., 2001; Stenman et al., 2003; Yun et al., 2003; Yoshihara et al., 2005). Thus, we used BrdU pulse/chase labeling to determine whether a significant population of cells is generated in the E14.5 ventral forebrain and migrates to the OB between midgestation and birth (Fig. 1). We counted the number of heavily labeled $BrdU^+$ cells in non-overlapping radial probes of the OB in 3 separate horizontal sections at each time point. 6 h after injection, $BrdU^+$ cells are most likely generated within the OB rudiment (1314 cells/$mm^2$; Fig. 1A). These cells may represent late-born mitral or early-born tufted cells (Hinds, 1968a). At E15.5, the density of $BrdU^+$ cells in the OB increases (1556 cells/$mm^2$; Fig. 1B), suggesting that a subset of labeled cells from distal locations have migrated into the OB. The density of $BrdU^+$ cells increases to a maximal level at E16.5 (2603 cells/$mm^2$). This suggests that the remaining E14.5-labeled $BrdU^+$ cells that will migrate to the OB have arrived by this time (see also Fig. 3). As the olfactory bulb continues to enlarge, the density of $BrdU^+$ cells declines (E17.5: 1728 cells/$mm^2$; Fig. 1C and P0: 1261 cells/$mm^2$; Fig. 1D). By P0, $BrdU^+$ cells are predominately located in the nascent granule and glomerular layers of the OB (Fig. 1D). To assess potential sources of this apparently migratory population of $BrdU^+$ cells, we examined sagittal sections through the developing forebrain. By E16.5, E14.5 $BrdU^+$ cells are found in a continuous cell-dense subventricular stream extending from the dorso-lateral LGE to the OB (Figs. 1E–G; arrowheads, Figs. 1A–B). Apparently, a relatively large population of cells, generated on E14.5, migrates in a distinct pathway that may represent the presumptive rostral migratory stream and accumulates in the nascent glomerular and granule cell layers of the OB.

### *Identity and stability of early generated cells in the OB*

Early generated cells in the OB may be transient, biased toward a particular laminar fate, or contribute to molecularly distinct subsets of interneurons. E14.5 $BrdU^+$ cells persist in the granule and glomerular layers of P21 and P60 mice (Figs. 2A–B), suggesting that at least some of these cells survive an early postnatal wave of apoptosis in the OB (Fiske and Brunjes, 2001; Saito et al., 2004). To better define the contribution of E14.5-generated cells to distinct neuronal populations, we evaluated the frequency and molecular identity of these cells in each layer of the mature OB. E14.5 $BrdU^+$ cells occupy all laminae at P21 (Figs. 2A, D, G); the majority (80%), however, are located in the glomerular and granule cell layers (Fig. 2C). Apparently, the contribution of early generated cells to glomerular and granule layer histogenesis exceeds previous estimates (Hinds, 1968a; Bayer, 1983).

We next analyzed the expression of 4 molecular markers of distinct interneuron classes: GABA, calretinin, calbindin, and tyrosine hydroxylase (TH). 28% (856 double-labeled cells/3019 $BrdU^+$ cells) of E14.5 $BrdU^+$ cells in the glomerular layer are double-labeled for GABA (Figs. 2D, E, R), 13% (251/1945) for calretinin (Figs. 2G–I, R), 8% (264/3447) for calbindin (Figs. 2L–N, R), and 5% (196/4127) for TH (Figs. 2O–Q, R). 53% (2387/4529) of $BrdU^+$ cells in the granule cell layer can be labeled for GABA (Figs. 2D, F, R), while only 3% (128/3770) express calretinin (Figs. 2G, J–K, R). BrdU-calretinin double-labeled cells in the mitral cell layer (9%; 41/474) may represent subsets of later-generated mitral cells (Qin et al., 2005) or displaced granule or short axon cells — especially since over half of the E14.5 $BrdU^+$ cells in the mitral layer co-label for GABA (337/628; Fig. 2R). Thus, a subset of molecularly diverse OB interneurons is generated on E14.5 and is retained at least through the third week of postnatal development.

### *Specific migration of cells from the LGE to the OB*

Genetic loss-of-function and in utero fate mapping studies clearly implicate the LGE as the primary extrinsic source of OB interneurons. Nevertheless, the initial migration of early generated cells from the LGE to the rudimentary OB has not been directly visualized or manipulated experimentally. Thus, we developed an organotypic culture assay that preserves the geometry of the developing telencephalon and facilitates visualization of migratory cells as well as embryological

Fig. 2. E14.5 $BrdU^+$ cells are retained in the postnatal OB and co-label with OB interneuron markers. (A) $BrdU^+$ cells are located throughout the OB at P21 (blue = all nuclei, green = BrdU). Box represents a single radial probe used for quantification (see Methods) and subsequent images. (B) $BrdU^+$ cells are retained in a similar distribution in the P60 OB. (C) Distribution of $BrdU^+$ cells in the P21 OB. (D) GABA (red) and BrdU (green) labeling in the P21 OB. (E–F) BrdU-GABA double-labeled cells (arrows) in the glomerular (E) and granule cell (F) layers. (G) Calretinin (CR; red) and BrdU (green) labeling in the P21 OB. (H–K) BrdU-CR double-labeled cells (arrows) in the glomerular (H, I) and granule cell (J, K) layers. (L) Calbindin (CB; red) and BrdU (green) labeling in the glomerular layer of the P21 OB. (M–N) BrdU-CB double-labeled cells (arrows). (O) Tyrosine hydroxylase (TH; red) and BrdU (green) labeling in the glomerular layer of the P21 OB. (P–Q) BrdU-TH double-labeled cells (arrows). (R) Percentage of $BrdU^+$ cells that co-label for GABA, CR, CB, and TH, in each layer of the OB at P21. Scale bar in panel A = 500 μm; scale bars in panels B, D, G, = 100 μm; scale bars in panels E, H = 25 μm. Scale bar in panel E applies to panel F; panel H applies to panels I–K, M–N, P–Q. ONL = olfactory nerve layer; GL = glomerular layer; EPL = external plexiform layer; MCL = mitral cell layer; GCL = granule cell layer.

analyses of precursor potential and fate (Figs. 3A, B). After 4 days in vitro, homotopically transplanted LGE cells migrate robustly from the rostral margin of the LGE in coherent streams that converge at the base of the OB rudiment (Figs. 3C–E), comparable to that seen for E14.5 BrdU$^+$ cells in vivo at E16.5 (see Fig. 1E). In the migratory path, these cells usually have

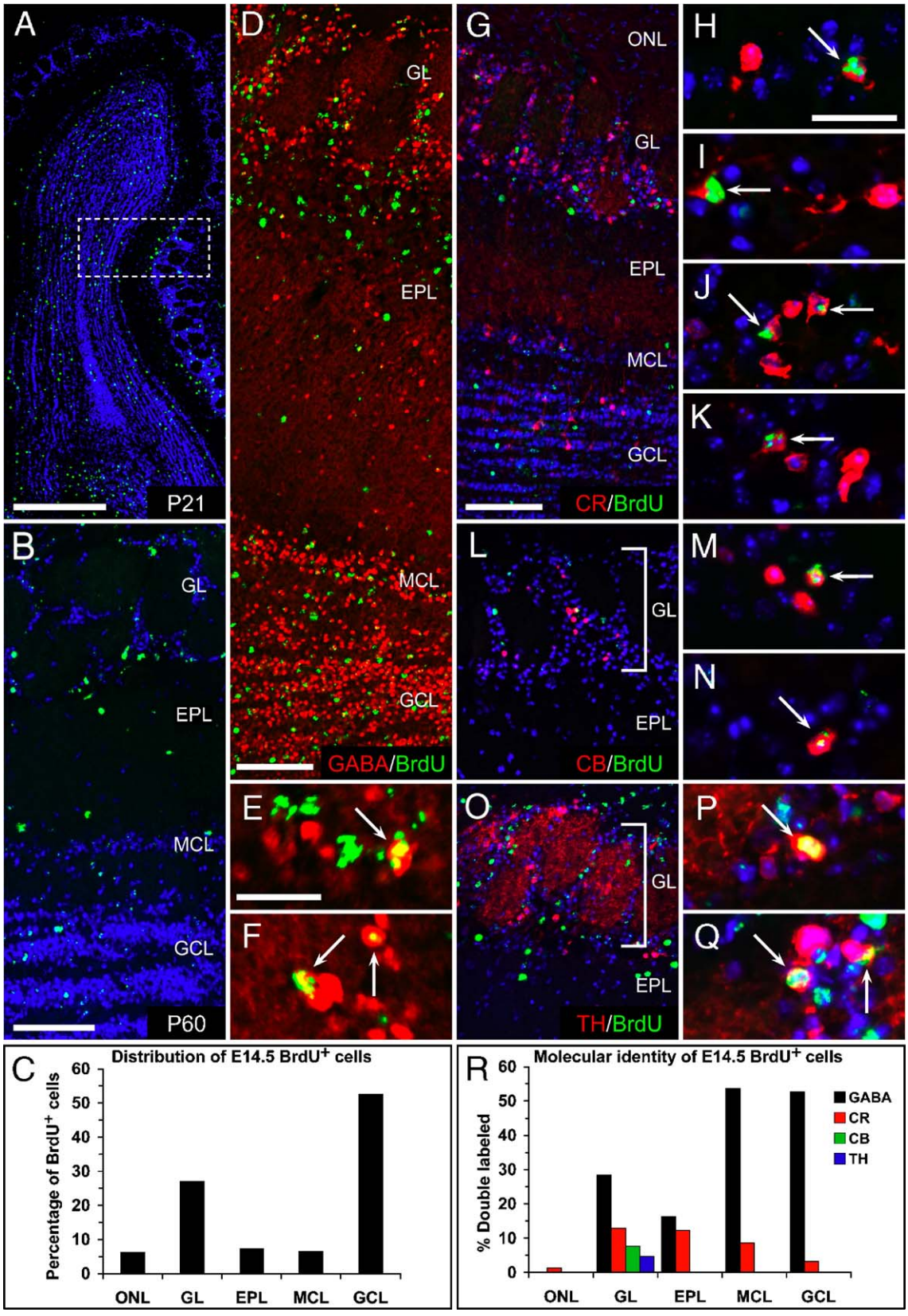

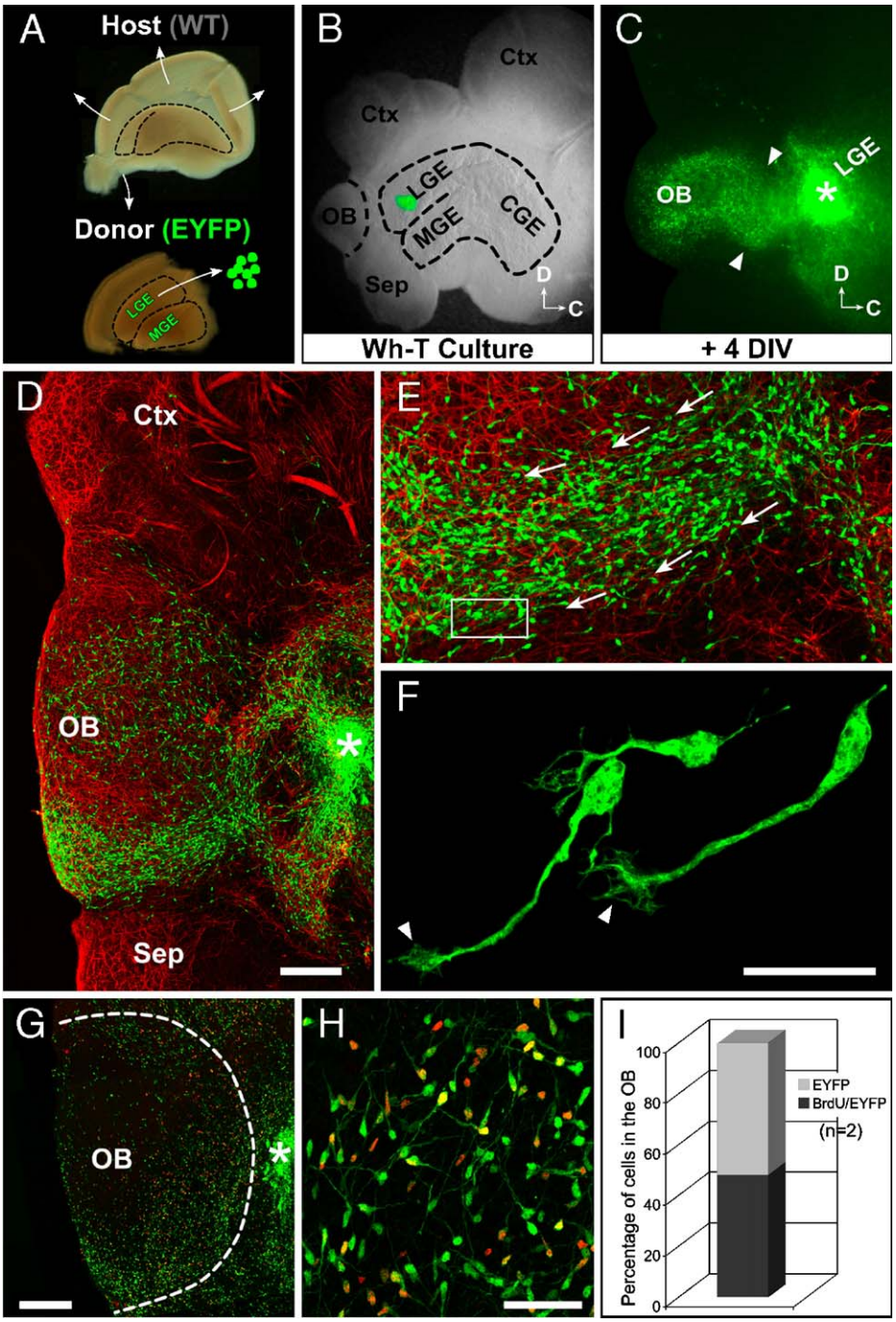


Fig. 3. E14.5 LGE-derived cells robustly migrate to the OB. (A–B) Donor (EYFP) LGE tissue is isolated and grafted into the LGE of a host (WT) telencephalon. (C) Fluorescence image of a living preparation grown 4 days in vitro (DIV); $EYFP^+$ cells migrate rostrally from the LGE graft site in a coherent stream (arrowheads). (D) Confocal montage of a fixed whole-mount preparation, grown 4 DIV, and stained for EYFP (green) and Tuj1 (red). Large numbers of LGE-derived cells selectively target the OB; migrating cells converge at the base of the OB rudiment. (E) Stream of LGE cells migrating rostrally (arrows) towards the OB. (F) LGE cells with migratory morphologies found at a position similar to box in panel E. Arrowheads indicate lamellate growth cones on two of the migratory LGE cells. (G–I) E14.5 $BrdU^+$ LGE cells migrate into the OB rudiment. BrdU was administered in vivo at E14.5, and EYFP/BrdU-exposed LGE tissue was grafted homotopically. After 4 DIV, nearly half (301/625) of the $EYFP^+$ cells (green) found in the OB co-label for BrdU (red). Scale bars in panels D and G = 200 μm; scale bar in panel F = 25 μm; scale bar in panel H = 50 μm. Asterisks = graft site; arrows in panel E indicate direction of migration; Wh-t = whole telencephalon.

small, fusiform cell bodies with leading processes that end in lamellate growth cones (Fig. 3F, arrowheads). The robust migration of homotopically transplanted E14.5 LGE cells into the OB is consistent with our BrdU data; nevertheless, our in vitro assay spans several days, and it is possible that migratory LGE cells are generated long after isolation and engraftment on E14.5. To determine if substantial numbers of migratory LGE cells destined for the OB are born on E14.5, we pre-labeled

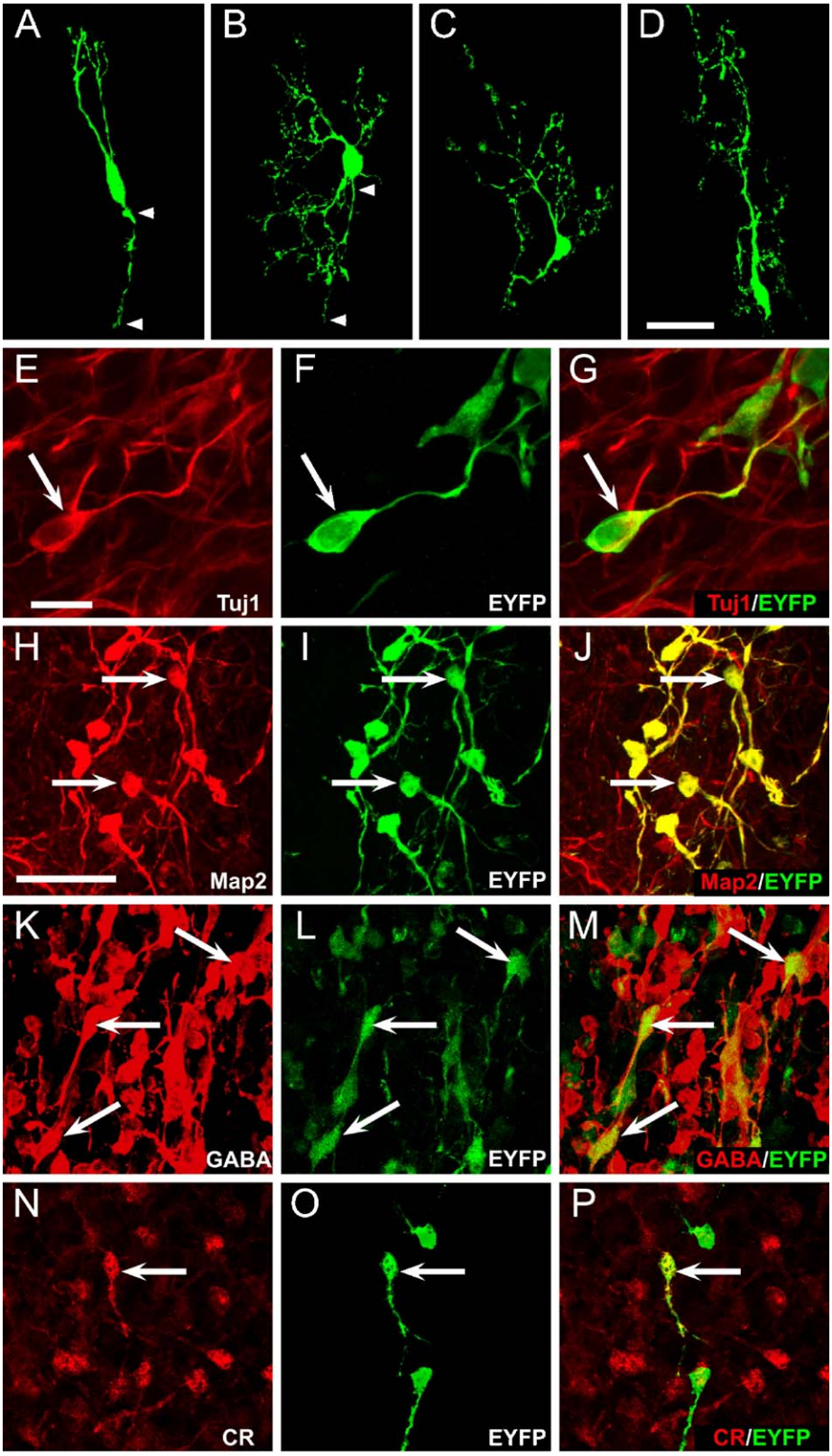


Fig. 4. LGE-derived cells display cellular and molecular hallmarks of OB interneurons in the OB rudiment. (A–D) LGE cells display a range of morphologies in the OB. (A–B) Some LGE cells have thin, unbranched apparent axons (arrowheads) and locally branched apparent dendrites. (C–D) Others have no morphologically apparent axon-like processes, but have long, branched apparent primary dendrites. (E–P) Molecular identity of LGE-derived cells. $EYFP^+$ LGE cells (green) express the early neuronal markers Tuj1 (E–G; red) and Map-2 (H–J; red), and the interneuron markers GABA (K–M; red) and calretinin (CR; N–P; red) in the OB rudiment. Scale bar in panel D = 20 μm, applies to panels A–C; scale bar in panel E = 10 μm; scale bar in panel H = 25 μm, applies to panels K, N.

donor embryos with a 1-h BrdU pulse followed by a thymidine chase, 2 h before harvesting and grafting. Approximately half (48%; 301/625) of the LGE-derived EYFP$^+$ cells in the OB were BrdU$^+$ (Figs. 3G–I). This reinforces our conclusion that significant numbers of E14.5-generated LGE–derived cells migrate specifically into the OB via a distinct pathway.

*Differentiation of OB interneurons and projection neurons*

A fundamental distinction among OB neurons is the differentiation of an axon. Periglomerular cells have short axons, granule cells lack axons entirely, and mitral cells develop long axons that coalesce into the lateral olfactory tract (LOT). Accordingly, we asked whether these cell biological distinctions reflect intrinsic identities of LGE versus OB precursors. In the OB rudiment in vitro, LGE-derived cells acquire a range of morphologies (Figs. 4A–D), some of which closely resemble mature OB interneurons. Some cells have multiple locally branched dendrites with an apparent fine caliber short axon (Figs. 4A, B, arrowheads) – similar to periglomerular cells – while others have an apparent primary locally branched dendrite with no recognizable axon (Figs. 4C, D)—cytological hallmarks of granule cells. In the OB rudiment in vitro, most LGE cells express Tuj1 (Figs. 4E–G) and Map-2 (Figs. 4H–J), markers of immature neurons, as well as GABA (Figs. 4K–M), the characteristic neurotransmitter of inhibitory interneurons. In addition, a subpopulation of LGE cells expresses calretinin (Figs. 4N–P), which labels both periglomerular and granule cells in vivo. Therefore, cells generated from LGE precursors in vitro at E14.5 acquire several diagnostic cytological and molecular features of OB interneurons.

We next asked whether cells from the OB rudiment are distinct from those in the LGE—particularly whether they, unlike their LGE counterparts that migrate to the OB, generate long axons. Cells in the OB rudiment of whole-telencephalon cultures have axons that coalesce into a coherent bundle resembling the LOT in vivo (Fig. 5A; Sato et al., 1998; Hirata et al., 2001; Lopez-Mascaraque et al., 2005). To distinguish the developmental potential of these cells versus those from the LGE, we grafted EYFP$^+$ OB tissue into the OB or LGE. OB cells do not appear to proliferate or migrate when grafted into either the OB or LGE (Figs. 5B–F). These OB-derived cells have irregularly shaped cell bodies with multiple neurites (Fig. 5E), even when grown in the LGE (Fig. 5D). Homotopically

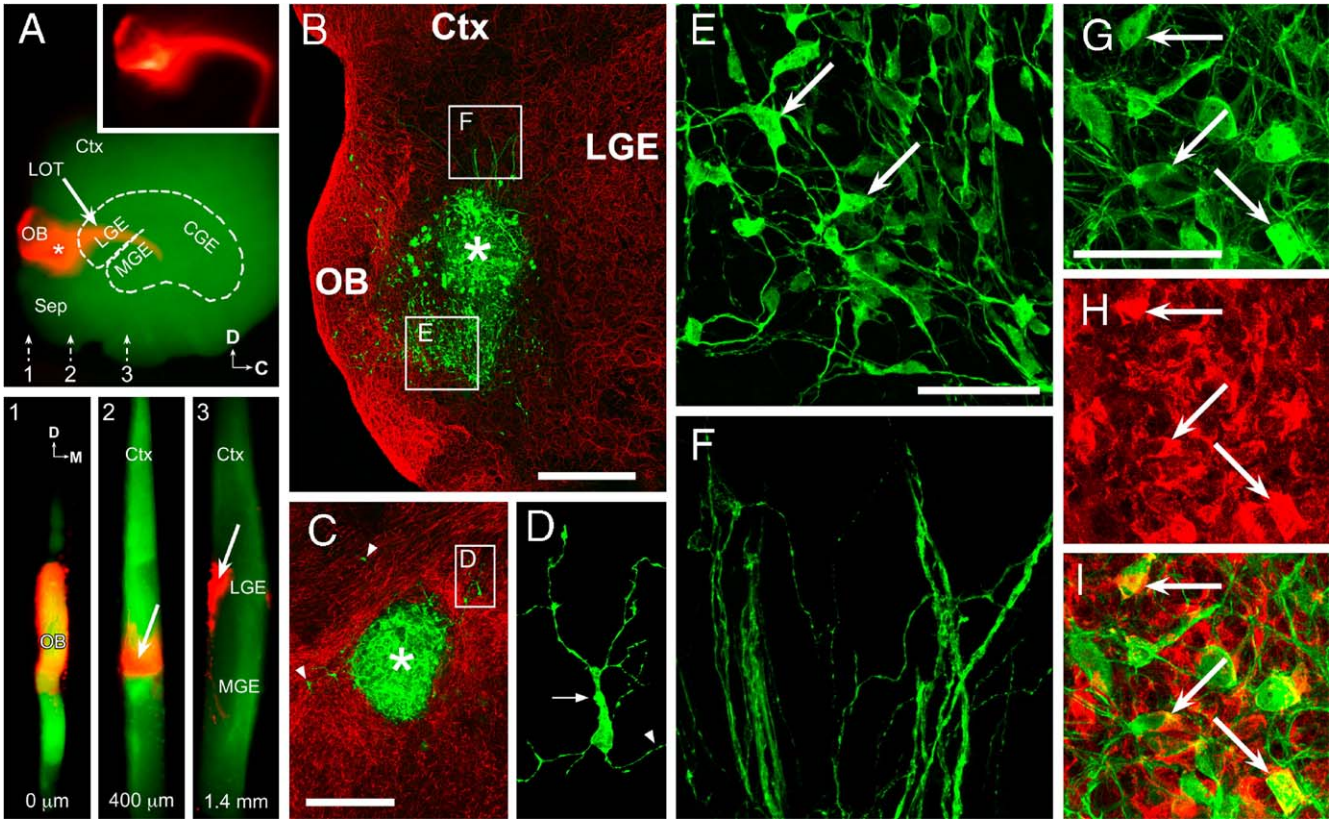


Fig. 5. OB cells are morphologically and molecularly distinct from contemporary LGE cells. (A) A crystal of DiI (asterisk) was placed into the OB of a whole telencephalon culture. Axons from labeled cells (inset) coalesce into a patent LOT. Coronal sections (1–3) of the DiI-labeled culture demonstrate the coherence of the LOT (arrows) in the ventro-lateral forebrain, in vitro. (B) Homotopically transplanted OB graft cells partially fill the OB rudiment and extend long axons, after 4DIV. (C) Cells (arrowheads) from OB graft do not migrate long distances when transplanted into the LGE. (D) High-magnification image of a differentiated OB-derived cell in the LGE (box in panel C) with a single primary dendrite (arrow) and apparent axon (arrowhead). (E) OB cells (arrows), from homotopically placed OB grafts (box in panel B), have irregularly shaped cell bodies and many neuritic processes. (F) High-magnification image of axon fascicles extending from OB graft (box in panel B). (G–I) OB-derived graft cells (arrows) co-label for HuC/D, which labels mitral cells in the adult OB. Scale bars = 400 µm in panel B, 200 µm in panel C, 50 µm in panels E, G. Width of panel D = 62 µm. Scale bar in panel E applies to panel F. Green = EYFP; red = DiI in panel A; Tuj1 in panel B; neurofilament-165 in panel C; HuC/D in panels H and I. Asterisks = graft site; LOT = lateral olfactory tract.

transplanted OB cells generate axon fascicles that project away from the OB rudiment (Figs. 5B, F). Many can be labeled for HuC/D (Figs. 5G–I), a neuron-associated RNA-binding protein seen selectively in mature mitral cells (Thompson Haskell et al., 2002). Apparently, E14.5 OB cells are distinct from LGE-derived cells. They express at least one mitral cell marker and

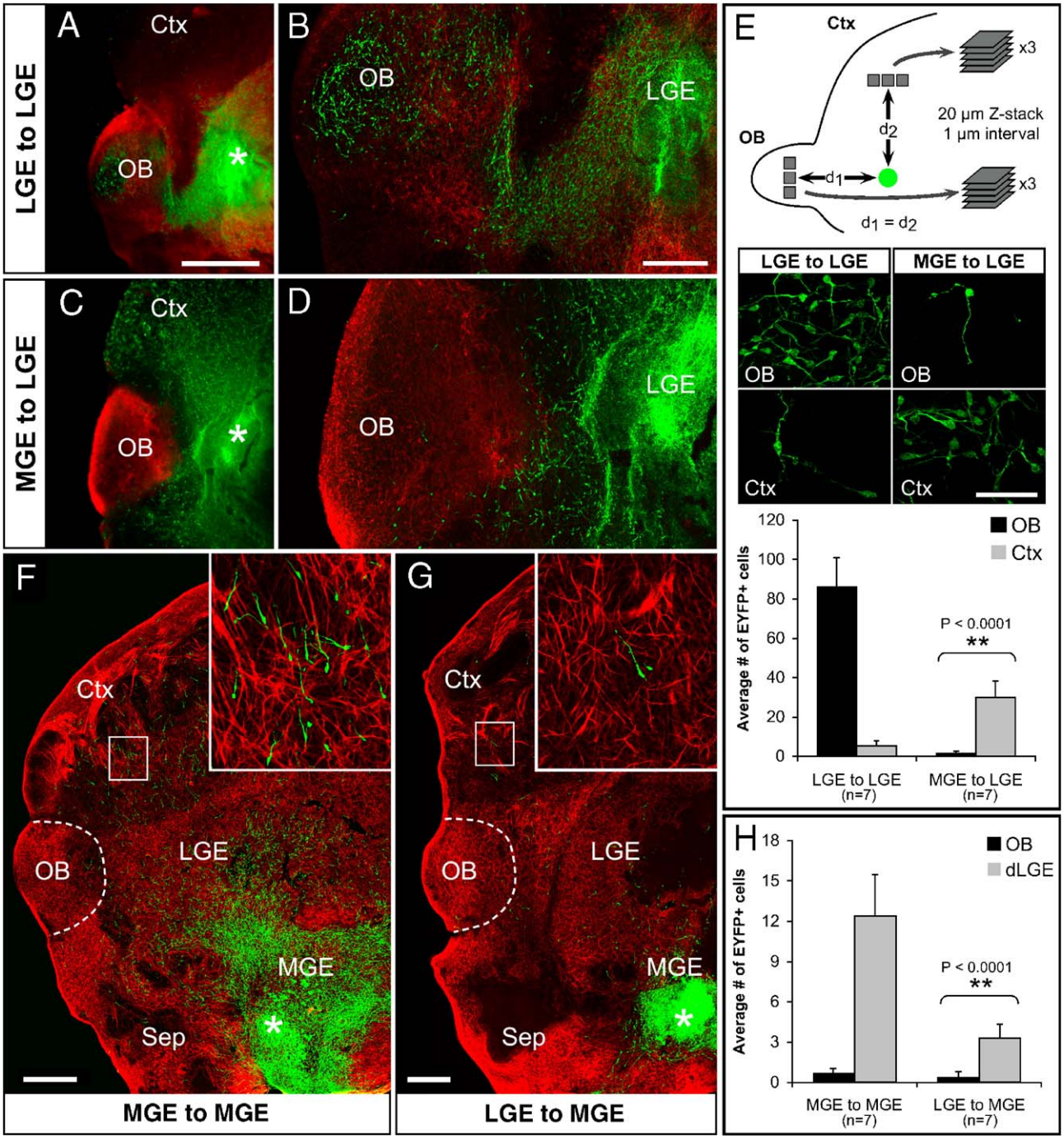


Fig. 6. LGE and MGE cells have distinct migratory specificities. (A–B) Homotopically transplanted LGE cells migrate extensively into the OB. (C–D) Heterotopically transplanted MGE cells migrate dorsally from the LGE, avoiding the OB. (E) Quantification of migratory specificity. Top panel: $EYFP^+$ cells are counted in 3 non-overlapping fields in the OB and Ctx. Middle panel: examples of $EYFP^+$ LGE (left) and MGE (right) cells in the OB and Ctx. Bottom panel: the number of $EYFP^+$ cells in the OB and Ctx is highly statistically different between LGE to LGE and MGE to LGE transplantation configurations (two-way ANOVA: $P < 0.0001$). (F) Homotopically transplanted MGE cells migrate dorsally through the LGE and accumulate in the cortex. Inset = enlargement of box showing MGE cells in the cortex. (G) LGE cells migrate short distances into the ventral forebrain when transplanted into the MGE and do not migrate in large numbers to either the cortex or OB. Inset: enlargement of box showing LGE cells in the cortex. (H) Migration from the MGE was quantified as above. The number of $EYFP^+$ cells differs significantly between MGE to MGE and LGE to MGE transplants (two-way ANOVA: $P < 0.0001$). Scale bars = 1 mm in panel A, 200 μm in panel B, 50 μm in panel E, and 400 μm in panels F and G. Scale in panel A applies to panel C, panel B applies to panel D. Asterisks = graft site. Green = EYFP; red = $GAD_{65}$ in panels A and B, calretinin in panels C and D, Tuj1 in panels F and G.

respond to local cues in the OB rudiment that promote axon extension.

*LGE and MGE cells have distinct migratory fates*

Fate mapping studies indicate that migratory LGE and MGE cells have distinct destinations (Anderson et al., 2001; Wichterle et al., 2001). Local signals or cell autonomous factors may determine the migratory capacity of LGE and MGE cells. To assess these mechanisms, we evaluated the migratory capacity and destinations of precursors grafted homologously or heterologously into the LGE and MGE. Non-forebrain precursors (e.g., E14.5 ventral spinal cord) incorporate in the host LGE but do not migrate far beyond the margins of the graft (data not shown). Apparently, the LGE environment does not confer migratory properties on dramatically heterologous tissue. In contrast, homotopically transplanted LGE cells migrate extensively into the OB rudiment (Figs. 6A, B; see also Figs. 3C, D). We next asked if MGE precursors migrate to the OB when placed in the LGE. MGE cells grafted into the LGE undergo robust tangential migration into the cortex; however, they almost completely avoid the OB (Figs. 6C, D). We confirmed this quantitatively and observed approximately 16× more LGE cells in the OB than the cortex in LGE to LGE transplants; similarly, there were 18× more MGE cells in the cortex than the OB for MGE to LGE transplants (Fig. 6E). When we compared the numbers of cells in the OB and cortex in each transplant configuration (two-way ANOVA: $P < 0.0001$), we found a significant statistical difference in the migratory destination of LGE versus MGE cells. Thus, migration of LGE cells to the OB is robust, quantifiable, and statistically distinct from that of MGE cells placed in the LGE environment.

We next asked whether LGE precursors behave similarly to their MGE counterparts when placed in the MGE, or whether they retain their migratory specificity for the OB. Homotopically transplanted MGE cells migrate to the cortex via routes that approximate those described previously both in vivo and in vitro (Fig. 6F; Anderson et al., 2001; Wichterle et al., 2001; Polleux et al., 2002; Yozu et al., 2005). LGE cells, when grafted ectopically in the MGE, primarily migrate dorsally into the striatum; very few cells reach either the OB or the cortex (Fig. 6G, and inset). We confirmed this by comparing numbers of cells in the dorsal LGE (dLGE) and OB in MGE to MGE and LGE to MGE transplants. In both cases, we observed significantly more cells in the dLGE than the OB (Fig. 6H; 17× difference for MGE to MGE, 8× difference for LGE to MGE). The numbers of cells in the dLGE versus the OB in MGE to MGE and LGE to MGE transplants were significantly different (two-way ANOVA: $P < 0.0001$). Thus, LGE cells placed in the MGE do not behave exactly like MGE cells, nor do they access or fully execute their normal migratory program to the OB.

It is possible that some of this apparent migratory specificity reflects instructive or inhibitory signals from the OB, cortex, or intervening migratory pathways. Direct apposition of LGE and MGE tissue with their quantitatively dominant targets, OB and cortex respectively, results in robust entry of migratory cells (Fig. 7, upper left and lower right). Reversed pairing, however, demonstrates a further distinction between LGE and MGE cells (Fig. 7, lower left and upper right). LGE cells do not migrate in substantial numbers into isolated cortical tissue, while MGE cells readily migrate into isolated OB tissue. Thus, LGE cells have a more limited capacity to enter potential forebrain targets than MGE cells.

*Developmental acquisition of migratory specificity*

LGE versus MGE migratory specificity may follow the morphogenetic and molecular differentiation of the ganglionic eminences between E11 and E15 (Bulfone et al., 1993; Corbin et al., 2000), or it may be established prior to the emergence of distinct LGE and MGE compartments. Accordingly, we asked whether ventral forebrain cells isolated from E9.5, 11.5, and 12.5 embryos – prior to or coincident with the emergence of the LGE and MGE – migrate specifically to the OB when placed in the E14.5 LGE (Fig. 8). E9.5 ventral forebrain epithelial (vFbE) cells, presumably including LGE progenitors, do not appear to migrate from the E14.5 LGE to any telencephalic location (data not shown; see Fig. 8H; $n = 10$). In contrast, when explants of E9.5-isolated vFbE are cultured intact for 2 days (Fig. 8A) and then placed into the E14.5 LGE, migration is seen in approximately 85% of our preparations (Figs. 8C, E, G; $n = 13$); nevertheless, there is no apparent specificity of these cells for the OB versus cortex. E9.5 vFbE cultured in the presence of frontonasal mesenchyme (FnM; Fig. 8B), which is

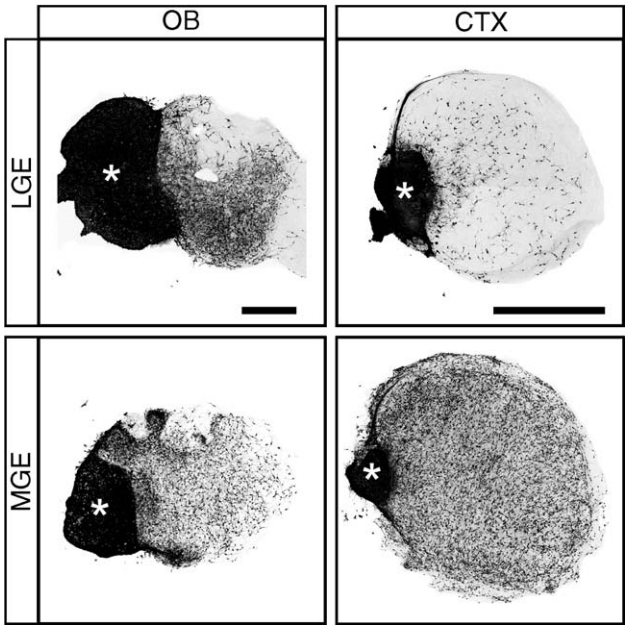


Fig. 7. Target selectivity differs between LGE and MGE cells. Top row. when directly apposed to their quantitatively dominant OB target (left), LGE cells migrate from the graft and invade the adjacent tissue. When LGE cells are paired with a cortical target (right), however, fewer LGE cells migrate from the graft into the cortical target tissue. Bottom row. MGE cells, when paired with an OB target (left), readily migrate into the inappropriate target tissue. When directly apposed to a cortical target (right), they migrate extensively into their appropriate target tissue. Scale bars = 400 μm. Scale bar in upper left applies to lower left; scale in upper right applies to lower right. Asterisks = grafts.

normally apposed to the lateral ventral forebrain in vivo, acquires an enhanced migratory capacity – without enhanced migratory specificity – that approximates that seen from E11.5 LGE grafts (Figs. 8G, H). Thus, early ventral forebrain cells autonomously acquire general migratory capacity between E9.5 and E11.5, prior to significant morphological differentiation of the ganglionic eminences. Furthermore, extrinsic signals from the frontonasal mesenchyme enhance this capacity.

Acquisition of LGE migratory specificity may proceed in parallel with additional morphogenetic and molecular differentiation of the LGE versus MGE. Morphogenesis of the MGE, which begins around E11.5, precedes that of the LGE by approximately 1 day. By E12.5, however, both structures are easily discernable. E12.5 LGE cells migrate less robustly from the E14.5 LGE environment than their E14.5 counterparts. Nevertheless, they are more frequently seen in the OB than the cortex (11× difference; Figs. 9A, C). In contrast, E12.5 MGE cells migrate robustly into the cortex and few are seen in the OB (8× difference; Figs. 9B, C). When the migratory behaviors of homotopic E12.5 LGE and heterotopic E12.5 MGE cells are compared (two-way ANOVA: $P < 0.0001$), they differ significantly in their target preference, as is the case at E14.5. Apparently, by E12.5, LGE cells have acquired their autonomous migratory preference for the OB and MGE cells have adopted a cortical migration program.

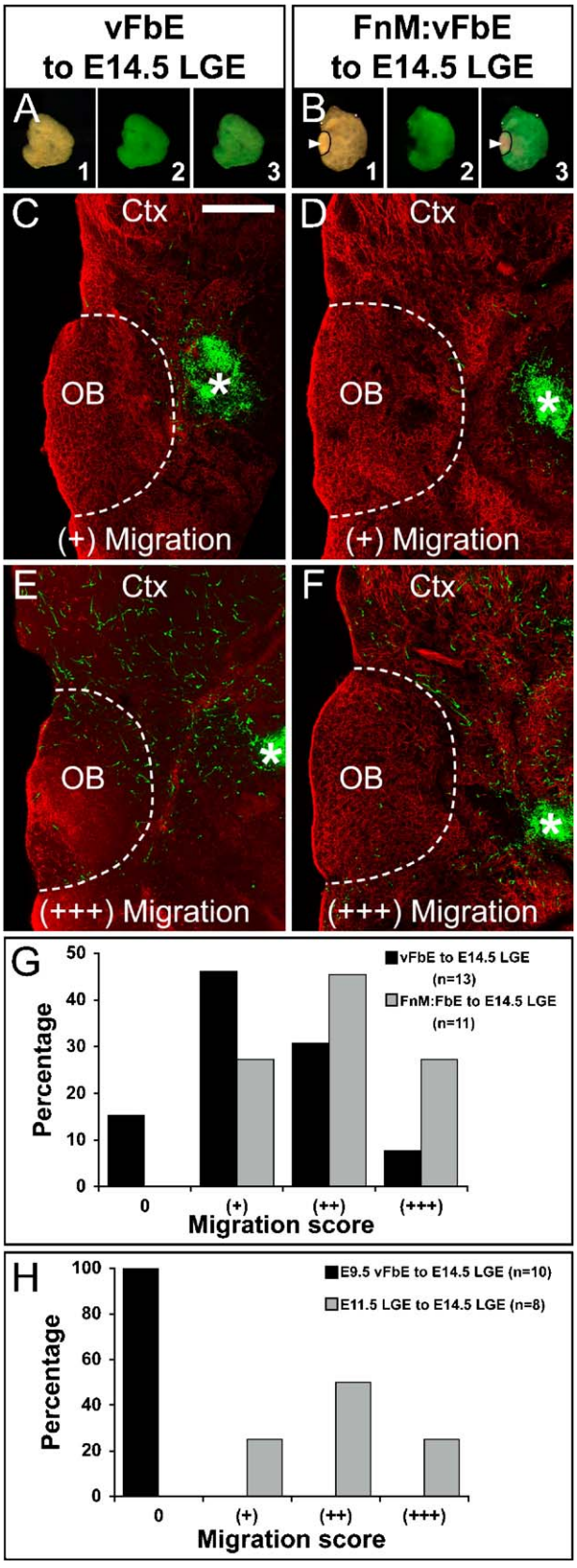


## Discussion

The earliest population of OB interneurons is generated primarily in the LGE, migrates into the rudimentary OB via a distinct pathway, accumulates in the nascent glomerular and granule cell layers, and differentiates into a cytologically and molecularly diverse group of interneurons. A novel in vitro assay allowed us to characterize the developmental specificity of this pioneering population of OB interneurons for the first time. The identity of their precursors reflects an apparent balance of cell autonomous factors established or reinforced by position in the LGE as early as E12.5, when the LGE becomes morphologically and molecularly distinct. The specific migration of LGE cells to the OB depends upon their initial location in the LGE. Cells from other locations can neither recognize nor follow this migratory pathway. These positionally specified LGE precursors and progeny likely constitute an antecedent of the postnatal subventricular zone (SVZ) and rostral migratory stream (RMS). Accordingly, cellular mechanisms that specify the earliest OB interneurons may concurrently establish a precursor niche that gives rise to migratory OB interneuron neuroblasts throughout life.

Fig. 8. Ventral forebrain precursors autonomously acquire the ability to migrate by E11.5. (A–B) EYFP$^+$ explants of E9.5 ventral forebrain epithelium (vFbE) were cultured for 2 DIV, either alone, or with unlabeled frontonasal mesenchyme (FnM:vFbE; arrowheads indicate mesenchymal tissue). (1) Bright field, (2) fluorescent, and (3) merged images of explant cultures. Explants were then grafted into the E14.5 LGE, grown for 4 DIV, and scored for migration (0 = no migration; + = least migration, +++ = most migration). (C–F) vFbE cells from vFbE (C, E) and FnM:vFbE explants (D, F) display a range of migration when grafted into the E14.5 LGE. (G) Distribution of migration scores from vFbE (2DIV) to LGE and FnM:vFbE (2DIV) to LGE transplants. (H) Distribution of migration scores from similarly assessed E9.5 vFbE (uncultured) to LGE and E11.5 LGE to LGE transplants. Scale bar in panel C = 200 μm, applies to panels D–F. Green = EYFP; red = Tuj1. Asterisks = graft site.

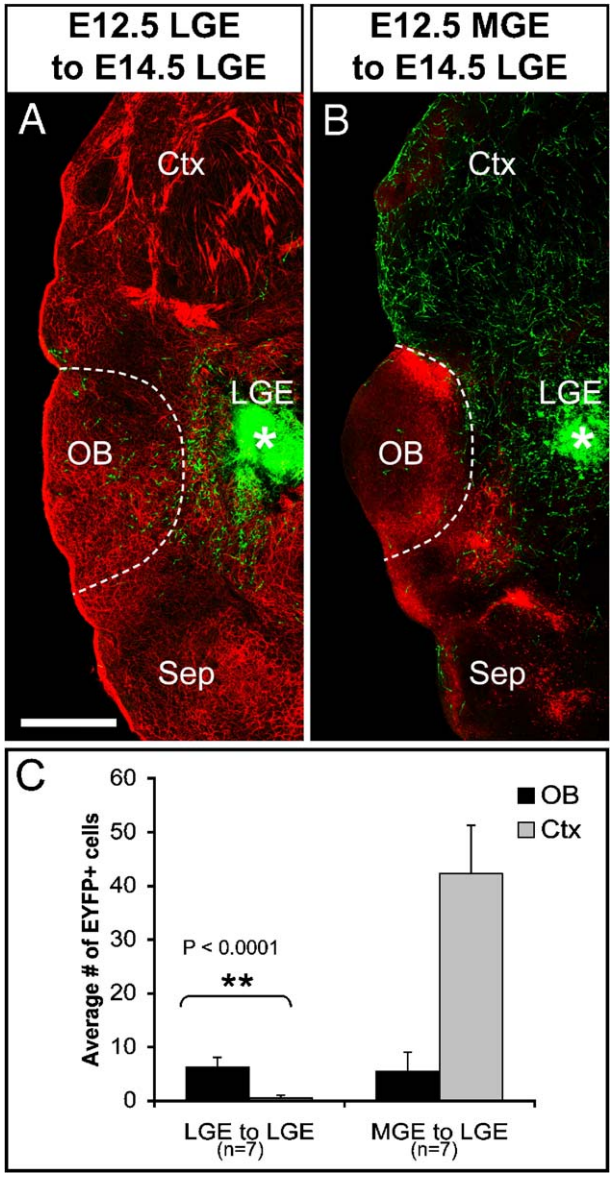


Fig. 9. Migratory specificity is established by E12.5. (A) E12.5 LGE cells transplanted into E14.5 LGE show limited migration; nevertheless, the cells preferentially target the OB. (B) E12.5 MGE cells transplanted into E14.5 LGE migrate dorsally into the cortex and avoid the OB, similar to E14.5 MGE cells. (C) The average number of cells in the cortex and OB from E12.5 LGE to E14.5 LGE transplants is statistically different from E12.5 MGE to E14.5 LGE transplants (two-way ANOVA: $P < 0.0001$). Scale bar in panel A = 500 μm, applies to panel B. Green = EYFP; red = Tuj1 in panel A, calretinin in panel B. Asterisks = graft site.

### *Studying early OB interneurons in vivo and in vitro*

Elegant in vivo lineage tracing experiments (Wichterle et al., 2001) as well as more recent neurochemical and electrophysiological analyses (Xu et al., 2004; Butt et al., 2005) provide insight into the derivation and differentiation of a broad range of forebrain interneurons, including those in the OB. Our in vivo BrdU labeling data extend and clarify many of these observations. Nevertheless, in vivo methods cannot easily generate the quantity and uniformity of experimental data necessary to evaluate precursor specificity, neuroblast migration, and intermediate steps in neuronal differentiation. Our in vitro assay allows rapid quantitative assessment of these mechanisms in the midgestation telencephalon. We found that forebrain regional architecture and development of long distance axon pathways is preserved in these preparations (see also Seibt et al., 2003). Using this assay, one can reproducibly and quantifiably vary the position, stage, and derivation of precursors, and monitor their subsequent migration and differentiation. Accordingly, we have been able to evaluate directly the relationship between time, position, and migratory specificity in the generation of OB versus other forebrain interneurons.

### *Embryonic genesis of OB interneurons*

The embryonic contingent of OB interneurons that we have characterized has largely been ignored, perhaps because previous studies indicate that most (>75%) are produced postnatally (Hinds, 1968a; Altman, 1969; Bayer, 1983). Our data likely underestimate the size of the earliest generated population since we limit BrdU exposure to 1 h on E14.5. Nevertheless, early generated cells are distributed widely in the OB, present in all layers, and comprise a molecularly diverse subset of GABA, calretinin, calbindin, and tyrosine hydroxylase (TH)-expressing interneurons (Gall et al., 1987; Kosaka et al., 1995; Kosaka et al., 1998) that are relatively insensitive to an early wave of OB cell death (Fiske and Brunjes, 2001; Saito et al., 2004). Accordingly, these cells may establish a stable scaffold for prolonged postnatal addition of OB interneurons (Altman, 1969; Bayer, 1983) and the corresponding construction of OB circuitry (Pomeroy et al., 1990). The prenatal arrival of these cells may impact key aspects of early OB development and subsequent function, including bulb growth, which is compromised by mutations that reduce OB interneuron numbers (Qiu et al., 1995; Anchan et al., 1997; Bulfone et al., 1998; Toresson and Campbell, 2001; Long et al., 2003; Yun et al., 2003), synaptogenesis, which begins at E15 (Hinds and Hinds, 1976; Hwang and Cohen, 1985), and early processing of odors, which is essential for initial feeding and parental imprinting in rodents (reviewed by McLean and Harley, 2004).

### *The LGE is the primary source of early OB interneurons*

We found that the LGE is the primary source of early generated OB interneurons. It has been suggested that many early OB cells – including interneurons – originate from epithelial precursors in the rudimentary OB itself (Hinds, 1968b; Gong and Shipley, 1995). The persistence of some bulb interneurons in *Dlx*1/2 mutants (Anderson et al., 1997), where the primary genetic lesion presumably compromises migration from the ganglionic eminences, seems consistent with this conclusion. Nevertheless, our observations suggest that most early generated OB interneurons are derived from the LGE, while precursors from the E14.5 OB rudiment primarily display cellular and molecular characteristics associated with mitral cells. Accordingly, we suggest that OB morphogenesis relies on

the coordination of two sequential processes: one that first specifies mitral cell precursors, presumably in the anterior dorso-lateral telencephalon, at a fairly early stage (E9–10; Jimenez et al., 2000; Nomura and Osumi, 2004), and one that later regulates the production and migration of interneurons from precursors in the LGE during midgestation. We found that LGE cells acquire the general ability to migrate between E9.5 and E11.5 but do not migrate specifically to the OB until E12.5. Therefore, this delay in OB migration may ensure the appropriate temporal pairing of interneuron arrival with the initial differentiation of postmitotic projection neurons in the embryonic OB.

### *A unique migratory trajectory for OB interneurons*

We provide direct evidence that a singular migratory pathway is established between the LGE and rudimentary OB during midgestation. LGE-generated neuroblasts selectively recognize this pathway, while MGE-generated cells and other heterologous cells do not. Previous observations indicate that an organized migratory domain exists between the ganglionic eminences and the rudimentary OB (Zerucha et al., 2000; Pencea and Luskin, 2003). It was not clear, however, whether this region constitutes a specific pathway for migratory cells generated in the LGE. We found that most migratory LGE cells do not stray far beyond the OB pathway, and most MGE cells do not recognize this apparent antecedent of the RMS. Indeed, LGE and MGE cells must travel in orthogonal trajectories within this domain to reach their respective targets. LGE cells seem to be more rigidly constrained in their migratory capacity than MGE cells. MGE cells can enter both the OB and cortex when placed directly next to either target, while LGE cells only robustly enter the OB in the same configurations. Apparently, a balance of attractive and inhibitory guidance cues, acting locally within the ventral forebrain and in the appropriate target field, establish distinct migratory trajectories for LGE and MGE cells. Thus, LGE-generated neuroblasts may preferentially recognize specific cues in the immature forebrain including Ig superfamily molecules, integrins, and members of the neuregulin family, whose expression remain enhanced in the adult RMS (Hu et al., 1996; Chazal et al., 2000; Murase and Horwitz, 2002; Anton et al., 2004).

### *Migratory specificity of LGE-generated neuroblasts*

We have shown that LGE precursors are intrinsically and autonomously programmed during a relatively brief period to recognize a specific migratory pathway to the rudimentary OB. Apparently, from this time onward, these cells retain this specificity — indeed, E14.5 LGE cells placed in the adult SVZ, migrate to the OB (Wichterle et al., 1999). The LGE environment does not confer migratory specificity to other cells during midgestation. LGE cells, however, must reside in the LGE before migrating to the OB. Apparently, cell autonomous identity reinforced by local signals is required for LGE cells to migrate selectively to the OB. There is a critical period between E11.5 and E12.5 when this selective migratory capacity is established in the LGE. Before this time, general migratory ability is acquired gradually, perhaps reflecting a balance of intrinsic factors in the ventral forebrain epithelium and extrinsic signals provided by adjacent frontonasal mesenchyme (LaMantia et al., 1993; Anchan et al., 1997; Xu et al., 2005). Commitment to specific migratory fates appears to be fairly rigid: once established, the migratory potential of LGE or MGE cells is not malleable. This question has been addressed for heterotopically transplanted MGE and CGE cells (Nery et al., 2002; Yozu et al., 2005), as well as for LGE cells transplanted into the MGE (Wichterle et al., 2001), and in each case, the transplanted cells do not adopt migratory characteristics of their host location. This suggests that precursors within the ventral telencephalon acquire identities that not only define neuronal subtypes (Fode et al., 2000; Parras et al., 2002; Schuurmans and Guillemot, 2002) but also ensure migratory fidelity.

### *Initial and ongoing specification of OB interneurons*

The genesis, migration, and differentiation of an initial compliment of stable OB interneurons from positionally-specified LGE precursors may represent the prenatal establishment of the progenitor niche – the SVZ – and migratory pathway – the RMS – for OB interneurons that persists through adulthood (Altman, 1969; Luskin, 1993; Lois and Alvarez-Buylla, 1994; Alvarez-Buylla and Garcia-Verdugo, 2002; Haskell and LaMantia, 2005). During development, the establishment of OB interneuron precursors in the LGE and the patterning of a distinct migratory pathway to the OB may represent two independent events: first, interneuron precursors in the LGE autonomously acquire their specific identity, then, LGE-derived neuroblasts uniquely recognize a migratory pathway to the OB. Accordingly, a combination of position, lineage, and selective migration during embryonic development may define regions of the adult brain that mediate ongoing replacement of OB interneurons. Our data show that these events occur with great temporal and spatial specificity for LGE precursors and their OB interneuron progeny. It remains to be determined what aspects of this specificity are preserved throughout life to facilitate the continued generation of OB interneurons.

## Acknowledgments

This work was supported by NIDCD postdoctoral fellowship DC007047 to E.S.T, a NARSAD young investigator grant to F.P., a NARSAD independent investigator grant to A.S.L., NINDS grant NS047701 to F.P., NICHD grant HD029178 to A.S.L., and NIMH grant MH64065 to A.S.L. The UNC Neuroscience Center Confocal Microscopy Core, which provided a resource for confocal imaging, was supported by NINDS grant NS031768. The authors thank Lance Brown, Hunter Councill, and Josh Smith for their excellent technical assistance, Clifford Heindel for mouse care and technical support, and Amanda Peters for laboratory management. Several antibodies used in this study were obtained from the Developmental Studies Hybridoma Bank.

## References


Altman, J., 1969. Autoradiographic and histological studies of postnatal neurogenesis: IV. Cell proliferation and migration in the anterior forebrain, with special reference to persisting neurogenesis in the olfactory bulb. J. Comp. Neurol. 137, 433–457.

Alvarez-Buylla, A., Garcia-Verdugo, J.M., 2002. Neurogenesis in adult subventricular zone. J. Neurosci. 22, 629–634.

Alvarez-Buylla, A., Lim, D.A., 2004. For the long run: maintaining germinal niches in the adult brain. Neuron 41, 683–686.

Anchan, R.M., Drake, D.P., Haines, C.F., Gerwe, E.A., LaMantia, A.S., 1997. Disruption of local retinoid-mediated gene expression accompanies abnormal development in the mammalian olfactory pathway. J. Comp. Neurol. 379, 171–184.

Anderson, S.A., Eisenstat, D.D., Shi, L., Rubenstein, J.L., 1997. Interneuron migration from basal forebrain to neocortex: dependence on Dlx genes. Science 278, 474–476.

Anderson, S.A., Marin, O., Horn, C., Jennings, K., Rubenstein, J.L., 2001. Distinct cortical migrations from the medial and lateral ganglionic eminences. Development 128, 353–363.

Anton, E.S., Ghashghaei, H.T., Weber, J.L., McCann, C., Fischer, T.M., Cheung, I.D., Gassmann, M., Messing, A., Klein, R., Schwab, M.H., Lloyd, K.C., Lai, C., 2004. Receptor tyrosine kinase ErbB4 modulates neuroblast migration and placement in the adult forebrain. Nat. Neurosci. 7, 1319–1328.

Bayer, S.A., 1983. 3H-thymidine-radiographic studies of neurogenesis in the rat olfactory bulb. Exp. Brain Res. 50, 329–340.

Bulfone, A., Puelles, L., Porteus, M.H., Frohman, M.A., Martin, G.R., Rubenstein, J.L., 1993. Spatially restricted expression of Dlx-1, Dlx-2 (Tes-1), Gbx-2, and Wnt-3 in the embryonic day 12.5 mouse forebrain defines potential transverse and longitudinal segmental boundaries. J. Neurosci. 13, 3155–3172.

Bulfone, A., Wang, F., Hevner, R., Anderson, S., Cutforth, T., Chen, S., Meneses, J., Pedersen, R., Axel, R., Rubenstein, J.L., 1998. An olfactory sensory map develops in the absence of normal projection neurons or GABAergic interneurons. Neuron 21, 1273–1282.

Butt, S.J., Fuccillo, M., Nery, S., Noctor, S., Kriegstein, A., Corbin, J.G., Fishell, G., 2005. The temporal and spatial origins of cortical interneurons predict their physiological subtype. Neuron 48, 591–604.

Chazal, G., Durbec, P., Jankovski, A., Rougon, G., Cremer, H., 2000. Consequences of neural cell adhesion molecule deficiency on cell migration in the rostral migratory stream of the mouse. J. Neurosci. 20, 1446–1457.

Corbin, J.G., Gaiano, N., Machold, R.P., Langston, A., Fishell, G., 2000. The Gsh2 homeodomain gene controls multiple aspects of telencephalic development. Development 127, 5007–5020.

Fiske, B.K., Brunjes, P.C., 2001. Cell death in the developing and sensory-deprived rat olfactory bulb. J. Comp. Neurol. 431, 311–319.

Fode, C., Ma, Q., Casarosa, S., Ang, S.L., Anderson, D.J., Guillemot, F., 2000. A role for neural determination genes in specifying the dorsoventral identity of telencephalic neurons. Genes Dev 14, 67–80.

Gall, C.M., Hendry, S.H., Seroogy, K.B., Jones, E.G., Haycock, J.W., 1987. Evidence for coexistence of GABA and dopamine in neurons of the rat olfactory bulb. J. Comp. Neurol. 266, 307–318.

Gong, Q., Shipley, M.T., 1995. Evidence that pioneer olfactory axons regulate telencephalon cell cycle kinetics to induce the formation of the olfactory bulb. Neuron 14, 91–101.

Haskell, G.T., LaMantia, A.S., 2005. Retinoic acid signaling identifies a distinct precursor population in the developing and adult forebrain. J. Neurosci. 25, 7636–7647.

Hinds, J.W., 1968a. Autoradiographic study of histogenesis in the mouse olfactory bulb: I. Time of origin of neurons and neuroglia. J. Comp. Neurol. 134, 287–304.

Hinds, J.W., 1968b. Autoradiographic study of histogenesis in the mouse olfactory bulb: II. Cell proliferation and migration. J. Comp. Neurol. 134, 305–322.

Hinds, J.W., Hinds, P.L., 1976. Synapse formation in the mouse olfactory bulb: I. Quantitative studies. J. Comp. Neurol. 169, 15–40.

Hirata, T., Fujisawa, H., Wu, J.Y., Rao, Y., 2001. Short-range guidance of olfactory bulb axons is independent of repulsive factor slit. J. Neurosci. 21, 2373–2379.

Hu, H., Tomasiewicz, H., Magnuson, T., Rutishauser, U., 1996. The role of polysialic acid in migration of olfactory bulb interneuron precursors in the subventricular zone. Neuron 16, 735–743.

Hwang, H.M., Cohen, R.S., 1985. Freeze-fracture analysis of synaptogenesis in glomeruli of mouse olfactory bulb. J. Neurocytol. 14, 997–1018.

Jimenez, D., Garcia, C., de Castro, F., Chedotal, A., Sotelo, C., de Carlos, J.A., Valverde, F., Lopez-Mascaraque, L., 2000. Evidence for intrinsic development of olfactory structures in Pax-6 mutant mice. J. Comp. Neurol. 428, 511–526.

Kosaka, K., Aika, Y., Toida, K., Heizmann, C.W., Hunziker, W., Jacobowitz, D.M., Nagatsu, I., Streit, P., Visser, T.J., Kosaka, T., 1995. Chemically defined neuron groups and their subpopulations in the glomerular layer of the rat main olfactory bulb. Neurosci Res 23, 73–88.

Kosaka, K., Toida, K., Aika, Y., Kosaka, T., 1998. How simple is the organization of the olfactory glomerulus? The heterogeneity of so-called periglomerular cells. Neurosci Res 30, 101–110.

LaMantia, A.S., Colbert, M.C., Linney, E., 1993. Retinoic acid induction and regional differentiation prefigure olfactory pathway formation in the mammalian forebrain. Neuron 10, 1035–1048.

LaMantia, A.S., Bhasin, N., Rhodes, K., Heemskerk, J., 2000. Mesenchymal/epithelial induction mediates olfactory pathway formation. Neuron 28, 411–425.

Lois, C., Alvarez-Buylla, A., 1993. Proliferating subventricular zone cells in the adult mammalian forebrain can differentiate into neurons and glia. Proc. Natl. Acad. Sci. U. S. A. 90, 2074–2077.

Lois, C., Alvarez-Buylla, A., 1994. Long-distance neuronal migration in the adult mammalian brain. Science 264, 1145–1148.

Long, J.E., Garel, S., Depew, M.J., Tobet, S., Rubenstein, J.L., 2003. DLX5 regulates development of peripheral and central components of the olfactory system. J. Neurosci. 23, 568–578.

Lopez-Mascaraque, L., Garcia, C., Blanchart, A., De Carlos, J.A., 2005. Olfactory epithelium influences the orientation of mitral cell dendrites during development. Dev. Dyn. 232, 325–335.

Luskin, M.B., 1993. Restricted proliferation and migration of postnatally generated neurons derived from the forebrain subventricular zone. Neuron 11, 173–189.

Marin, O., Anderson, S.A., Rubenstein, J.L., 2000. Origin and molecular specification of striatal interneurons. J. Neurosci. 20, 6063–6076.

McLean, J.H., Harley, C.W., 2004. Olfactory learning in the rat pup: a model that may permit visualization of a mammalian memory trace. NeuroReport 15, 1691–1697.

Murase, S., Horwitz, A.F., 2002. Deleted in colorectal carcinoma and differentially expressed integrins mediate the directional migration of neural precursors in the rostral migratory stream. J. Neurosci. 22, 3568–3579.

Nery, S., Fishell, G., Corbin, J.G., 2002. The caudal ganglionic eminence is a source of distinct cortical and subcortical cell populations. Nat. Neurosci. 5, 1279–1287.

Nomura, T., Osumi, N., 2004. Misrouting of mitral cell progenitors in the Pax6/small eye rat telencephalon. Development 131, 787–796.

Parras, C.M., Schuurmans, C., Scardigli, R., Kim, J., Anderson, D.J., Guillemot, F., 2002. Divergent functions of the proneural genes Mash1 and Ngn2 in the specification of neuronal subtype identity. Genes Dev. 16, 324–328.

Pencea, V., Luskin, M.B., 2003. Prenatal development of the rodent rostral migratory stream. J. Comp. Neurol. 463, 402–418.

Pleasure, S.J., Anderson, S., Hevner, R., Bagri, A., Marin, O., Lowenstein, D.H., Rubenstein, J.L., 2000. Cell migration from the ganglionic eminences is required for the development of hippocampal GABAergic interneurons. Neuron 28, 727–740.

Polleux, F., Ghosh, A., 2002. The slice overlay assay: a versatile tool to study the influence of extracellular signals on neuronal development. Sci. STKE L9.

Polleux, F., Whitford, K.L., Dijkhuizen, P.A., Vitalis, T., Ghosh, A., 2002. Control of cortical interneuron migration by neurotrophins and PI3-kinase signaling. Development 129, 3147–3160.

Pomeroy, S.L., LaMantia, A.S., Purves, D., 1990. Postnatal construction of neural circuitry in the mouse olfactory bulb. J. Neurosci. 10, 1952–1966.

Qin, Z.P., Ye, S.M., Du, J.Z., Shen, G.Y., 2005. Postnatal developmental expression of calbindin, calretinin and parvalbumin in mouse main olfactory bulb. Acta Biochim. Biophys. Sin. (Shanghai) 37, 276–282.

Qiu, M., Bulfone, A., Martinez, S., Meneses, J.J., Shimamura, K., Pedersen, R. A., Rubenstein, J.L., 1995. Null mutation of Dlx-2 results in abnormal morphogenesis of proximal first and second branchial arch derivatives and abnormal differentiation in the forebrain. Genes Dev. 9, 2523–2538.

Rosselli-Austin, L., Altman, J., 1979. The postnatal development of the main olfactory bulb of the rat. J. Dev. Physiol. 1, 295–313.

Saito, K., Saito, S., Taniguchi, K., Kobayashi, N., Terashita, T., Shimokawa, T., Mominoki, K., Miyawaki, K., Chen, J., Gao, S.Y., Li, C.Y., Matsuda, S., 2004. Transient increase of TUNEL-positive cells on postnatal day 20 in the developing rat olfactory bulb. Neurosci. Res. 50, 219–225.

Sato, Y., Hirata, T., Ogawa, M., Fujisawa, H., 1998. Requirement for early-generated neurons recognized by monoclonal antibody lot1 in the formation of lateral olfactory tract. J. Neurosci. 18, 7800–7810.

Schuurmans, C., Guillemot, F., 2002. Molecular mechanisms underlying cell fate specification in the developing telencephalon. Curr. Opin. Neurobiol. 12, 26–34.

Seibt, J., Schuurmans, C., Gradwhol, G., Dehay, C., Vanderhaeghen, P., Guillemot, F., Polleux, F., 2003. Neurogenin2 specifies the connectivity of thalamic neurons by controlling axon responsiveness to intermediate target cues. Neuron 39, 439–452.

Stenman, J., Toresson, H., Campbell, K., 2003. Identification of two distinct progenitor populations in the lateral ganglionic eminence: implications for striatal and olfactory bulb neurogenesis. J. Neurosci. 23, 167–174.

Thompson Haskell, G., Maynard, T.M., Shatzmiller, R.A., Lamantia, A.S., 2002. Retinoic acid signaling at sites of plasticity in the mature central nervous system. J. Comp. Neurol. 452, 228–241.

Toresson, H., Campbell, K., 2001. A role for Gsh1 in the developing striatum and olfactory bulb of Gsh2 mutant mice. Development 128, 4769–4780.

Wichterle, H., Garcia-Verdugo, J.M., Herrera, D.G., Alvarez-Buylla, A., 1999. Young neurons from medial ganglionic eminence disperse in adult and embryonic brain. Nat. Neurosci. 2, 461–466.

Wichterle, H., Turnbull, D.H., Nery, S., Fishell, G., Alvarez-Buylla, A., 2001. In utero fate mapping reveals distinct migratory pathways and fates of neurons born in the mammalian basal forebrain. Development 128, 3759–3771.

Xu, Q., Cobos, I., De La Cruz, E., Rubenstein, J.L., Anderson, S.A., 2004. Origins of cortical interneuron subtypes. J. Neurosci. 24, 2612–2622.

Xu, Q., Wonders, C.P., Anderson, S.A., 2005. Sonic hedgehog maintains the identity of cortical interneuron progenitors in the ventral telencephalon. Development 132, 4987–4998.

Yoshihara, S., Omichi, K., Yanazawa, M., Kitamura, K., Yoshihara, Y., 2005. Arx homeobox gene is essential for development of mouse olfactory system. Development 132, 751–762.

Yozu, M., Tabata, H., Nakajima, K., 2005. The caudal migratory stream: a novel migratory stream of interneurons derived from the caudal ganglionic eminence in the developing mouse forebrain. J. Neurosci. 25, 7268–7277.

Yun, K., Potter, S., Rubenstein, J.L., 2001. Gsh2 and Pax6 play complementary roles in dorsoventral patterning of the mammalian telencephalon. Development 128, 193–205.

Yun, K., Garel, S., Fischman, S., Rubenstein, J.L., 2003. Patterning of the lateral ganglionic eminence by the Gsh1 and Gsh2 homeobox genes regulates striatal and olfactory bulb histogenesis and the growth of axons through the basal ganglia. J. Comp. Neurol. 461, 151–165.

Zerucha, T., Stuhmer, T., Hatch, G., Park, B.K., Long, Q., Yu, G., Gambarotta, A., Schultz, J.R., Rubenstein, J.L., Ekker, M., 2000. A highly conserved enhancer in the Dlx5/Dlx6 intergenic region is the site of cross-regulatory interactions between Dlx genes in the embryonic forebrain. J. Neurosci. 20, 709–721.